Pergamon

Bioorganic & Medicinal Chemistry 6 (1998) 2013–2027

BIOORGANIC & MEDICINAL CHEMISTRY

Design and Synthesis of Nonpeptide Angiotensin II Receptor Antagonists Featuring Acyclic Imidazole-mimicking Structural Units

Mauro Angiolini,[a] Laura Belvisi,[a] Davide Poma,[b] Aldo Salimbeni,[b] Nunzio Sciammetta[a] and Carlo Scolastico[a]*

[a]*University of Milano, Organic and Industrial Chemistry Department, C.N.R. Centre for the Study of Organic and Natural Compounds, via Venezian 21, I-20133 Milano, Italy*

[b]*Lusofarmaco,† Medicinal Chemistry Department, via Carnia 26, I-20132 Milano, Italy*

Received 5 March 1998; accepted 2 June 1998

Abstract—Extensive molecular modelling studies, including conformational analysis and the comparison of molecular electrostatic potential distributions, were used to evaluate structural parameters of new antagonists containing acyclic replacements of the N=C-N imidazole region. The synthesis and the biological screening of a series of acyl biphenyltetrazole derivatives were planned and realized to gain an insight into the structure–activity relationships of this unusual class of Angiotensin II antagonists.

Introduction

The search for Angiotensin II (AII) receptor antagonists as potential antihypertensive agents started more than 20 years ago and many peptidic antagonists have been described in the literature.[1] The discovery by the Du Pont group of a series of (biphenylmethyl)imidazoles as nonpeptidic, potent and orally active AII receptor (AT_1 subtype) antagonists has opened up a completely new field in AII antagonist research, and structure–activity relationships for this class of compounds have been intensively explored.[2]

The most representative structure in the series is Losartan[3] (DuP-753, Fig. 1), which is already employed for the treatment of hypertension in man. A variety of nonpeptide AII receptor antagonists have been reported over the last few years,[4] and modifications of this lead compound have been attempted. As already outlined in a previous paper,[5] reports on the efficient replacement of the biphenyltetrazole moiety are scarce, especially in the imidazole series.

By contrast a number of studies have appeared in which the imidazole moiety of DuP-753 is successfully replaced by other five-or six-membered ring heterocycles (one or more fused) indicating that the AII receptor is quite permissive in accepting this region of the nonpeptide antagonists. Examples of these imidazole-mimicking groups that maintain high affinity for the AT_1 receptor include imidazopyridine, benzimidazole, quinoline, pyrazole, triazole, pyrimidine and pyrimidinone.

Potent, orally active, AT_1 selective AII receptor antagonists containing a pyrimidinone ring that carries a C-linked biphenyltetrazole moiety and an arylmethyl group on the N-3-position were recently discovered by our group.[6] Milfasartan (LR-B/081, Fig. 2), one of the most potent compounds in vitro and in vivo in the series,[7] was developed and subjected to clinical evaluation for the treatment of hypertension. Powerful tools in addressing the design process were our prior knowledge of the geometric and electrostatic requirements for AII receptor binding[8,9] and the results of overlay studies employing a computationally-derived AII model.

Key words: Antihypertension; antagonists; molecular modelling.
*Corresponding author. Tel.: 0039 2 2367593; fax: 39 2 2364369; e-mail scola@iumchx.chimorg.unimi.it
†Company related to A. Menarini, Industrie Farmaceutiche Riunite.

0968-0896/98/$ - see front matter
PII: S0968-0896(98)00160-6

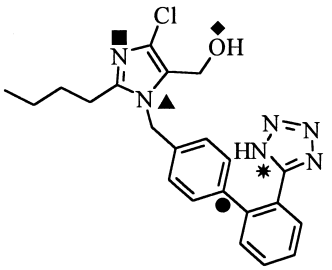

DuP-753 (Losartan)

Figure 1. Compound Dup-753 (Losartan). The labelled atoms have been considered in the definition of conformational descriptors.

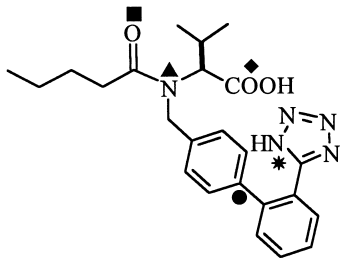

CGP48933 (Valsartan)

Figure 3. Aminoacid-derived antagonist CGP48933 (Valsartan). The labelled atoms have been considered in the definition of conformational descriptors.

The imidazole was also efficiently replaced by suitable acyclic structural units: for example the amide group O=C–N was found to be a good substitute for the N=C–N imidazole region. Valsartan (CGP48933, Fig. 3) is the lead compound of a structurally unique series of highly potent antagonists discovered by Ciba–Geigy where the heterocycle of Losartan has been replaced by an N-acylated aminoacid residue.[10]

Following these results, a series of novel molecules were designed as potential AII antagonists (Fig. 4), our aim being to explore acyclic structural alternatives to the tetra-substituted imidazole of DuP-753 while preserving the optimum (1*H*-tetrazol-5-yl)biphenyl moiety. As structure–activity relationships in this field are lacking, we projected the study of geometrical and electrostatic properties, the synthesis and the testing of representative compounds to verify the validity of previously determined binding requirements to the AT_1 receptor.[8,9]

Molecular modelling

In our study the potent aminoacid-derived antagonist Valsartan (Fig. 3) was adopted as the acyclic reference compound. Its geometrical and interaction energy properties have already been investigated within the framework of a 3-D QSAR CoMFA study performed on a training set of 28 nonpeptide AII antagonists.[11] Consistency of the CoMFA model with the previously derived geometric and electrostatic pharmacophoric hypotheses[8,9] was observed. The antagonist Valsartan fully agreed with the proposed activity models, fulfilling all binding requirements, as will be shown later.

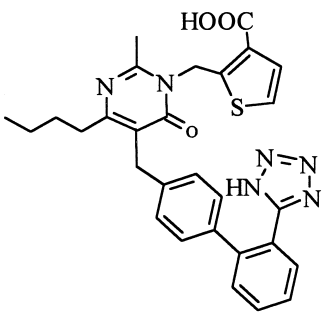

LR-B/081 (Milfasartan)

Figure 2. Compound LR-B/081 (Milfasartan).

The conformational and electrostatic characteristics of compounds **1a–6** (Fig. 4) were then analyzed and compared with the existing pharmacophoric patterns.

Conformational analysis

We had already performed a three-dimensional quantitative structure–activity relationships study on nonpeptide AII (AT_1) receptor antagonists, with the aim of identifying the 3-D geometrical requirements for receptor binding. By the combined use of conformational analysis and chemometrics we carried out a comparative analysis of the 3-D conformational features of 13 antagonists showing different levels of binding affinity, and defined the spatial functionality relationships necessary for activity.[8] Interatomic distances between atoms belonging to relevant moieties common to all the training set molecules were adopted as 3-D geometrical molecular descriptors. Figure 1 shows the pharmacophoric points for compound DuP-753. The values of these descriptors, adopted by only the AII antagonists showing the highest levels of receptor affinity, were searched for and then considered to characterize the 'active conformation(s)' (i.e. the conformation(s) in which the molecules interact at the receptor site).

The structure–activity relationship between the interatomic distances and the biological activity was assessed by using the linear discriminant classification tree (LDCT) method.[12] A geometrical model in the form of a multivariate decision tree was obtained, where three

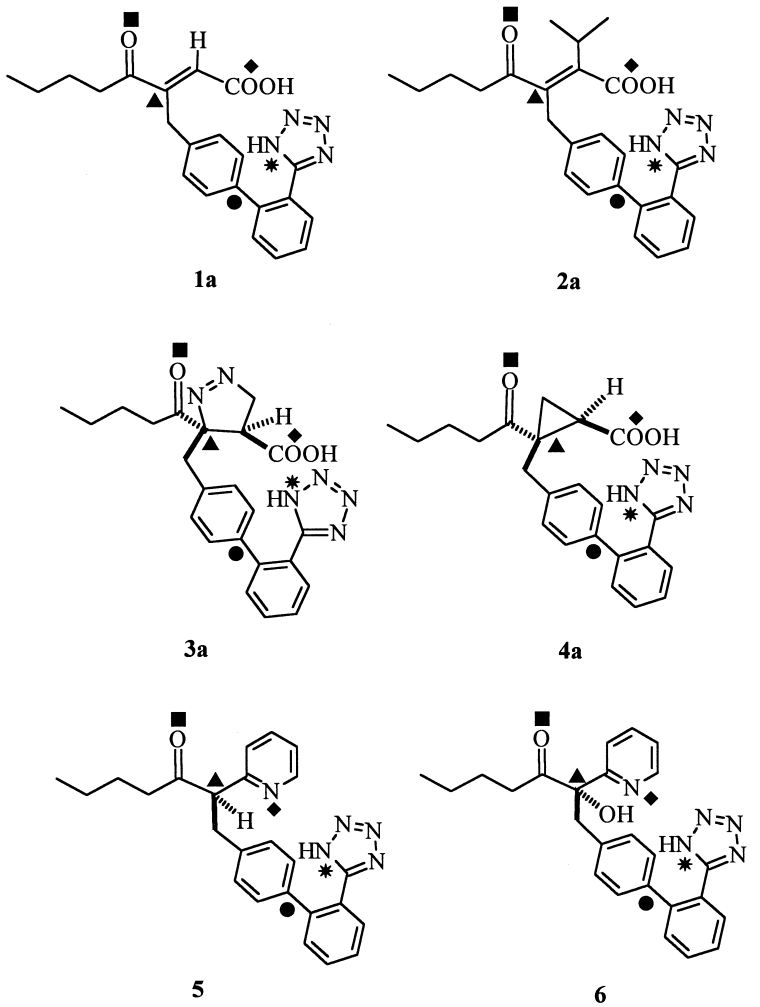

Figure 4. Acyclic derivatives **1a–6**. The labelled atoms have been considered in the definition of conformational descriptors.

significantly different putative active geometries can be identified.[8]

As for the training set AII antagonists, the conformational analysis of compounds **1a–6** and Valsartan was carried out performing in vacuo molecular mechanics calculations, randomly varying torsional space. The usage-directed Monte Carlo conformational search,[13] the MM2* force field,[14] and the TNCG energy minimization algorithm[15] implemented in the MacroModel V3.1X and the BatchMin V3.1 programs[16] were used to find the conformational minima within an 8 kcal/mol energy cutoff.[17] These conformers were then classified by the geometrical activity model on the basis of the values assumed by the selected interatomic distances in each of them. The pharmacophoric points considered for the definition of conformational descriptors in acyclic molecules are shown in Figures 3 and 4.

The LDCT method not only permits the classification of unknown compounds but can also establish the reliability of the prediction by verifying the existence of similarity between the variables' values of the tested molecules and those of the training set AII antagonists. The discriminant function, linear combination of all the variables (interatomic distances), that permits the maximum separation between the two groups is searched for. If poor separation between tested compounds and training set antagonists is observed, geometrical homogeneity and reliability of the prediction could be concluded; otherwise, if the separation is complete, geometrical diversity and uncertainty in the prediction should be considered.

The percentage of conformers of the new molecules classified as active by the tree model and an indication of their actual similarity to training set geometries are

reported in Table 1. All the minima of Valsartan and compounds **3a**, **4a**, **5** and **6** closely agreed with the interatomic distance 3-D QSAR model, placing relevant functional groups exactly as in the more active training set antagonists. Lower activity percentages were obtained for compounds **1a** and **2a** (84% and 65%, respectively), together with the indication that the arrangement of their pharmacophoric moieties is somewhat different from that of both active and inactive training set antagonists. As the LDCT model necessarily assigns the conformers of the tested compounds to a class, the training set active geometries were the closest ones to most of conformers of compounds **1a** and **2a** in the multidimensional descriptor space considered.

Molecular electrostatic potential

By means of a comparative analysis of the Molecular Electrostatic Potential (MEP) distributions of several simplified AII receptor antagonists, characterized by different binding affinities, we found that the electrostatic behaviour of the region surrounding the heterocycle is relevant for receptor interaction.[9]

The following electrostatic potential characteristics appear to be required for the recognition process: (a) a positive long-range MEP in the region of space surrounding the lipophilic side-chain and (b) strongly electrophile attracting regions bulging out of the heterocycle –N= type nitrogen atom and the hydrogen bond acceptor moiety placed at the side of the heterocyclic ring. The possibility of electrostatic discrimination among antagonists is related more to the overall topology of the electrostatic potential distributions in the regions of interest than to the depth (i.e. absolute value) of the MEP minima.

The N-acylated aminoacid residue of Valsartan displays all the topological MEP characteristics indicated as necessary for AII receptor recognition (Fig. 5): a positive potential region around the butyl chain and very deep negative zones around the amide carbonyl moiety and the carboxylic group.

As was previously performed on simplified DuPont antagonists, MEP distributions were computed from an ab initio wave function with a 3-21G basis set on simplified structures (Fig. 6) derived from the MM2* minimum energy conformations of the corresponding AII antagonists, using the GAUSSIAN 90[18] software package. 2-D isopotential maps in the plane containing the O1 = C2-N3 or the O1 = C2-C3 atoms (plane A) and in the parallel planes 1.7 Å below and above plane A (planes B and B′, not shown) were constructed by means of an interpolation technique with the SURFER program.[19]

In particular, the geometry of each fragment to be used for MEP calculations has been derived from the antagonists' lowest energy conformer that ensures the best superimposition of the relevant moieties of acyclic structural unit to the corresponding ones of the imidazole

Table 1. Predictions of the geometrical activity model and observed biological activity

Compound	% Geometrical Activity[a]	Similarity[b]	AII Binding[c] K_i (μM)
Valsartan	100	yes	0.0077
1a	84	no	1.5
2a	65	no	—
3a	100	yes	> 100
4a	100	yes	> 100
5	100	yes	43.1
6	100	yes	54.9

[a] Percentage of conformers classified as active by the tree model.

[b] This column describes if similarity exists between the conformers of the new molecules and those of the training set compounds.

[c] Inhibition of specific binding of [^{3}H]AII to rat adrenal cortical membranes (AT_1 receptors). Losartan: 0.011 μM; Milfasartan: 0.0014 μM.

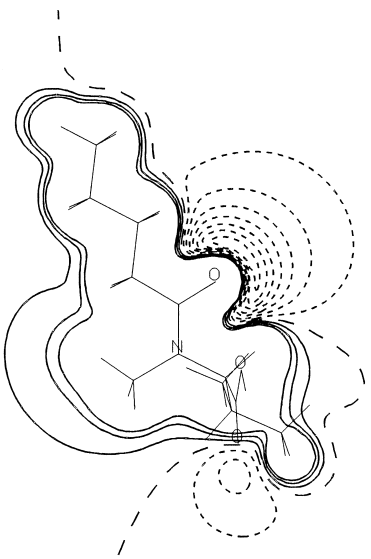

Figure 5. 2-D isopotential map for the N-acylated aminoacid residue of Valsartan (reference fragment) in plane A obtained with ab initio calculations with a 3-21G basis set. Isopotential contour interval: 10 kcal/mol. Negative and zero contours: short and long dashed lines, respectively; positive contours: solid lines. Only regions with potential < 30 kcal/mol are mapped. Minimum contour: −70 kcal/mol.

nucleus. The principal problem encountered is connected with the planar geometry imposed by the heterocyclic ring: only the amide group of Valsartan maintains the planarity of the structural core bearing the other key features. The results of conformational analysis show that derivatives **1a–6** present deviations from planarity for the acyl central region, the most significant being that observed in the α,β-unsaturated carbonyl compound **2a**.

Therefore, the geometries adopted for MEP calculation are characterized by the following absolute values for the torsion O1 = C2–C3–C4: about 60° for the fragment **F2** and about 30° for the remaining ones. MEP distributions in plane A for fragments **F1–F6** are reported in Figures 7–12.

The analysis of the 2-D isopotential maps reveals that the new acyclic fragments possess all the topological MEP characteristics indicated as necessary for AII receptor recognition: a positive potential region around the butyl chain and very deep negative zones around the carbonyl moiety and the other hydrogen-bond acceptor group. However, a number of doubtful points emerge from examination of MEP distributions produced by fragments **F2**, **F3**, and **F6**. Negative and zero contours, extending towards the aliphatic chain, appear in the middle-lower left of the map. This negative region, which is lacking in the isopotential maps of active reference antagonists (DuP-753 or Valsartan), is to be attributed to nonplanar conformation of the α,β-unsaturated carbonyl group in compound **2a**, to the pyrazole ring of compound **3a** and to the hydroxylic substituent of compound **6**.

As analogous topological MEP features have never been observed, neither in high-affinity nor low-affinity AII receptor antagonists, reliable predictions about electrostatic behaviour of compounds **2a**, **3a** and **6** cannot be formulated.

Despite the uncertainty sometimes resulting from the analysis of geometric and electrostatic properties of the new acyclic derivatives, we synthesized and tested some compounds, with the aim of gaining insight into the structure–activity relationships of acyclic diphenyltetrazole antagonists and checking the validity of previously derived binding requirements to the AT_1 receptor.

Chemistry

Diethyl methylphosphonate **7**[20] was treated with n-BuLi in dry THF at −78 °C under nitrogen. Ethyl valerate was added to achieve diethyl 2-oxo-hexylphosphonate **8** which was then deprotonated by the reaction with NaH in dry THF and alkylated with 5-[4′-(bromomethyl)-[1,1′-biphenyl]-2-yl]-1-(triphenylmethyl)-1*H*-tetrazole **9**[2] (BrMBTT) to prepare phosphonate **10** (Scheme 1).

The α,β-unsaturated esters **11** and **12** were synthesized by the Horner–Emmons condensation[21] between the sodium salt of phosphonate **10** and ethyl glyoxylate[22] in dry THF under nitrogen at room temperature. The products **11** and **12** were isolated in a 60/40 ratio (86% yield) by flash column chromatography (Scheme 2). The *Z*-isomer **12** shows a positive NOE between the benzylic methylene group and the olefinic hydrogen atom.

The removal of the N-trityl protective group was performed by heating a solution of **11** in methanol to give **1b**, in quantitative yield.

In the synthesis of the pyrazoline[23] **13**, the mixture of **11** and **12** was directly treated with diazomethane in Et_2O at −10 °C for 15 min until a yellow colour appeared. Only the *E*-isomer **11** reacted and after 2 h at room temperature the reaction mixture was evaporated and the residue chromatographed to isolate racemic pyrazoline **13**. The removal of the triphenylmethyl protecting group was performed by heating the solution of **13** in methanol to give **3b** (Scheme 3) quantitatively.

The successful conversion of pyrazoline **13** to the cyclopropane[24] derivative **14** was achieved in hexane/acetone 99/1 by 2 h irradiation with a medium pressure lamp (500 W). Using this procedure, nitrogen extrusion and carbon–carbon bond formation proceeded largely with retention of configuration of the pyrazoline **13**.

Two isomeric cyclopropanes derivatives were isolated and separated in 9/1 ratio (yield 53%) by flash column chromatography. The removal of the N-trityl protective group from the major isomer was obtained by heating in methanol to afford **4b** (Scheme 4) quantitatively.

The synthesis of pyridine derivatives **5**, **6** and **20** is shown in Schemes 5 and 6. The ketone **16** was obtained

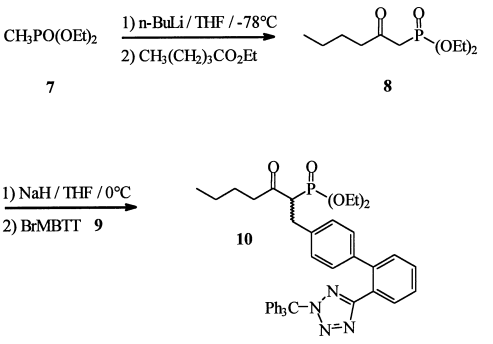

Scheme 1.

by 2-picoline and valeraldehyde condensation and subsequent oxidation with Jones's reagent.

The alkylation of the active methylenic group of **16** with 5-[4′-(bromomethyl)-[1,1-biphenyl]-2-yl]-1-(triphenylmethyl)-1*H*-tetrazole **9** was performed using NaH in THF to give the racemic intermediate **17** in high yield.

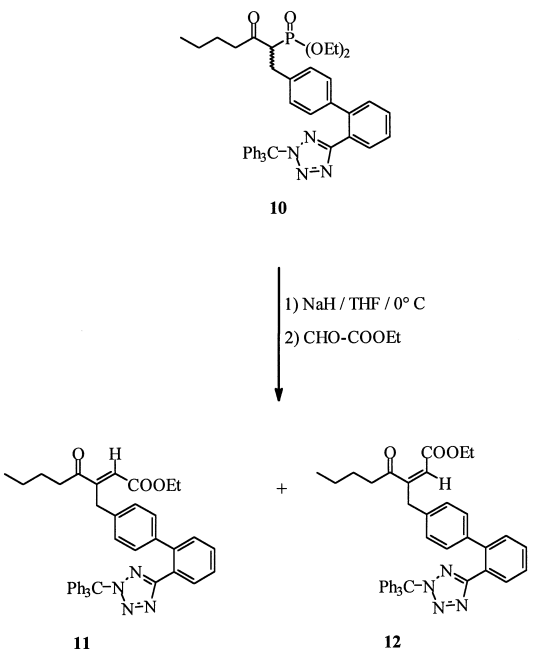

Scheme 2.

The subsequent reaction with *m*-chloroperbenzoic acid yielded the corresponding N-oxide **18** in a mixture with hydroxy derivative **19** in a 1/2 ratio, which were easily separated by flash-chromatography.

The NMR studies agreed with the structures. At $\delta = 5.99$ the ^{1}H NMR spectrum of **19** showed, unlike the **18** one, a singlet that exchanged with D_2O, corresponding to the hydroxy group. At the same time the disappearance of the peak at $\delta = 4.53$, corresponding to the hydrogen linked to the carbon between carbonyl and pyridine ring, was also observed.

Furthermore, the structures were confirmed by ^{13}C NMR studies performed on the corresponding trityl-deprotected derivatives **20** and **6**. The spectra of **20** and **6** showed the presence of a tertiary carbon at $\delta = 53.1$ and a quaternary carbon at $\delta = 83.5$, respectively. One hypothesis to explain the formation of compound **19** could be the epoxidation of the enolic form of **17**, followed by ring opening and the subsequent conversion into ketol **19**.

Finally, the target compounds were obtained by the removal of trityl group by refluxing with MeOH.

Discussion

The newly synthesized compounds were examined in vitro as AII antagonists by evaluating their ability to displace [^{3}H]AII from rat adrenal cortical membranes (RACM) as a source of AT_1 receptor.[6]

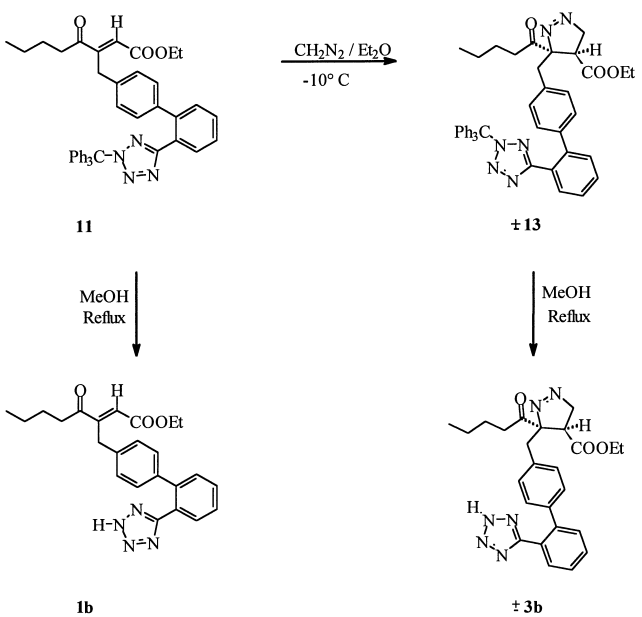

Scheme 3.

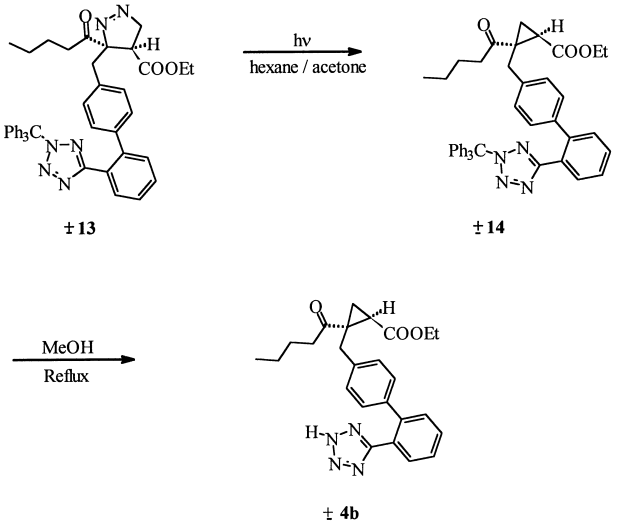

Scheme 4.

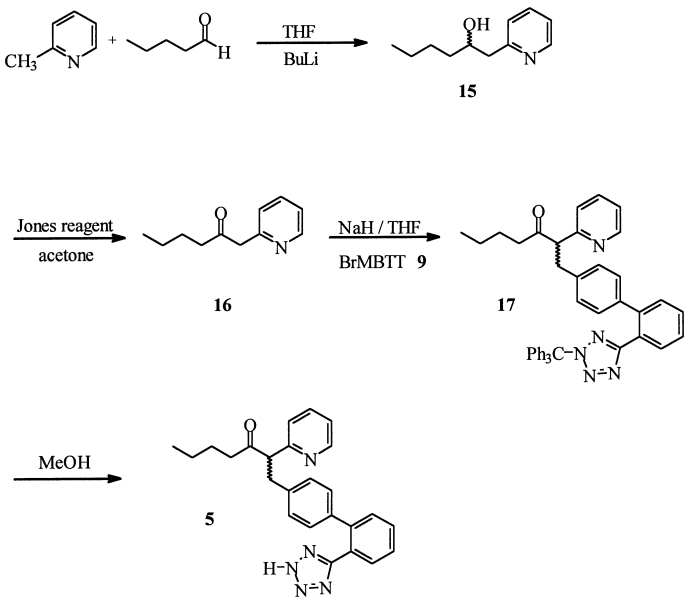

Scheme 5.

Compared to the reference DuPont (Losartan) or Ciba–Geigy (Valsartan) compounds, all the acyclic derivatives showed a significantly reduced potency: binding affinities in the μM range were observed instead of the nM values exhibited by the lead antagonists (Table 1).

Attempts to explain the influence on the activity of the structural changes on the heterocycle-mimicking moiety were performed by considering the results of the extensive molecular modelling studies, which took into consideration the conformational and electrostatic features of some of these compounds.

Replacement of the imidazole ring of DuP-753 or the amide moiety of Valsartan with an α,β-unsaturated carbonyl group was shown to have a profound effect on the overall conformation of the molecules and to produce 3-D structures which poorly align their pharmacophoric elements to the corresponding ones in known AII antagonists. The lack of geometrical similarity to training

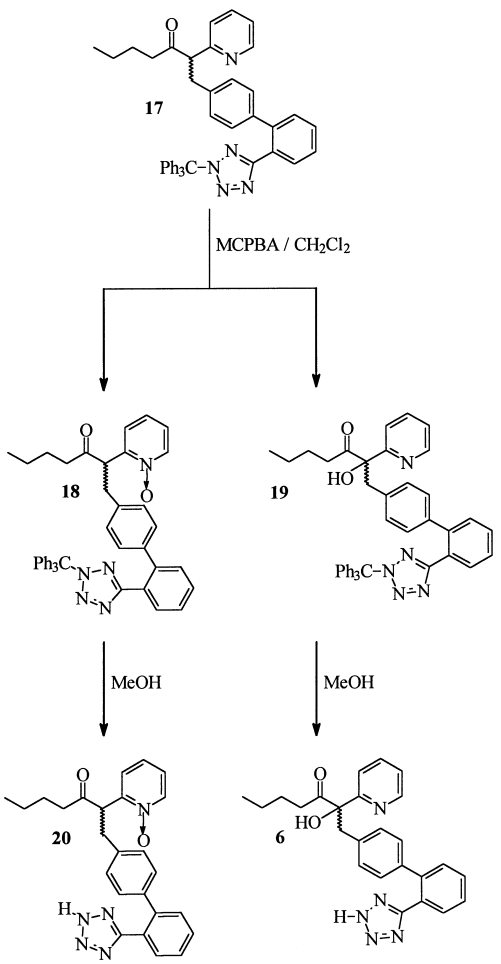

Scheme 6.

set (active or inactive) compounds observed for derivatives **1a** and **2a** (Table 1) leads to an uncertain, unpredictable situation, which does not necessarily imply lack of activity.

Unfortunately, pharmacological assays seem to suggest that the novel spatial functionality arrangement explored by α,β-unsaturated carbonyl derivatives is unsuitable for receptor binding. Electrostatic properties of these acyclic units could also be responsible for the observed lower activity, especially when the conformation of the α,β-unsaturated carbonyl group is characterized by a marked deviation from planarity. In this case, a negative isopotential region appears (see the map of fragment **F2** in Figure 8) which has no correspondence in the MEP distributions of known antagonists.

The other acyclic structural units allow pharmacophoric arrangements quite similar to those of high-affinity AII antagonists. However, the activity of these compounds was not comparable to that of the DuPont or Ciba–Geigy leads. This could be explained by hypothesizing that the acyclic structural units of compounds **3–6** possess charge distributions, which give rise to unfavourable interactions with the receptor.

As already observed, MEP distributions of the fragments **F3** and **F6** are characterized by the presence of negative isopotential contours approaching the butyl chain in the middle-lower left of the map. Although identical MEP patterns have never been observed in maps of known antagonists, the overall topology of the long-range negative MEP distribution around the aliphatic chain was shown to be critical in discriminating between active and inactive antagonists.[9]

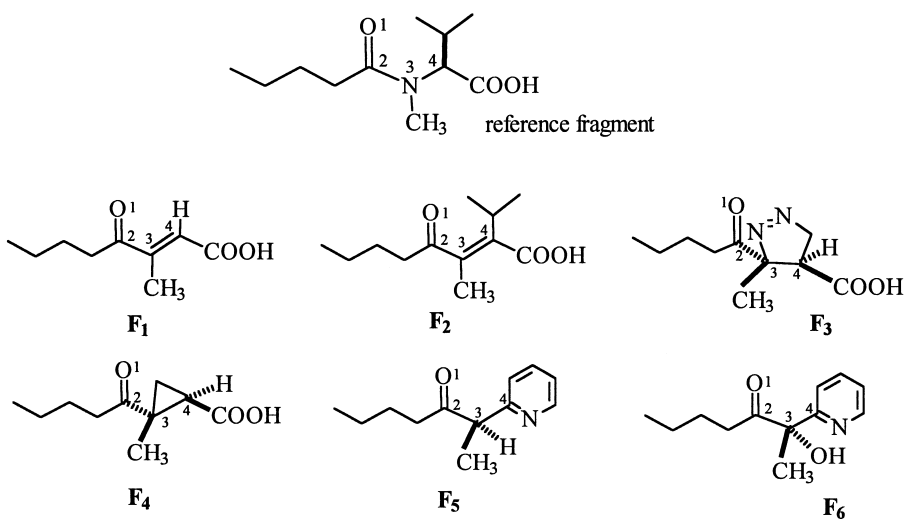

Figure 6. Molecular fragments, whose MEP distributions have been analyzed.

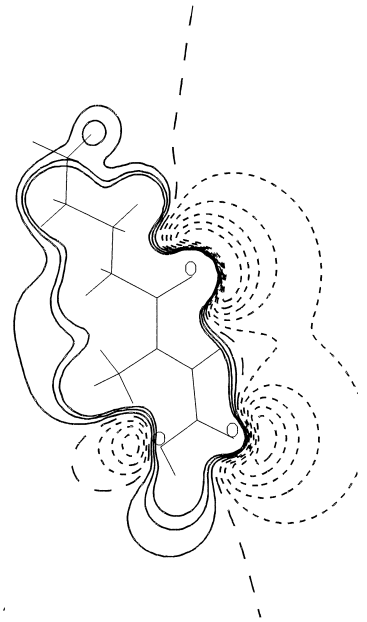

Figure 7. 2-D isopotential map for the fragment **F1** in plane A obtained with ab initio calculations with a 3-21G basis set. Contour details are as in Figure 5. Minimum contour: −50 kcal/mol.

The isopotential maps in the plane of the heterocycle of previously investigated low-affinity DuPont compounds were characterized by negative lines extending from the imidazole –N= atom to the upper left quadrant and by an isolated negative region of reduced dimensions in the middle left of the map.[9]

Following these considerations and the proximity of this electrophile-attractive region to the novel one observed in the maps of acyclic fragments, it could be hypothesized that molecular charge distributions of compounds **3a** and **6** in the space around the butyl substituent do not present the right requirements to fit well the aliphatic chain into a lipophilic pocket at the receptor site.

Charge distributions quite similar to those of lead compounds were observed for fragments **F4** and **F5**. However, it is worth noting that the conformation of the acyclic unit adopted for MEP calculations was suitably chosen so as to ensure the lowest deviation from planar geometry of the heterocycle or the amide group. MEP distributions generated by other conformations should be considered to complete the description of the electrostatic behaviour of these fragments.

As an example, the isopotential map in plane A of the structure derived from the lowest energy minimum conformation of compound **5** (with torsion angle O1=C2–C3–C4 of about 120°) is reported in Figure 13. The

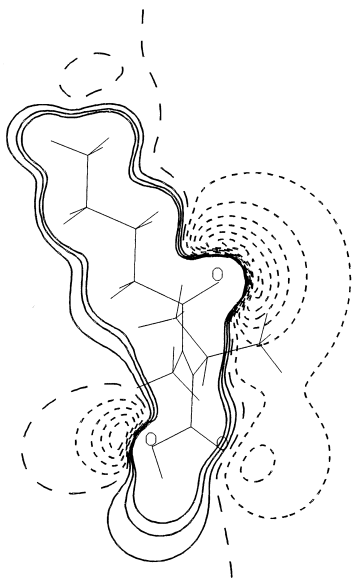

Figure 8. 2-D isopotential map for the fragment **F2** in plane A obtained with ab initio calculations with a 3-21G basis set. Contour details are as in Figure 5. Minimum contour: −60 kcal/mol.

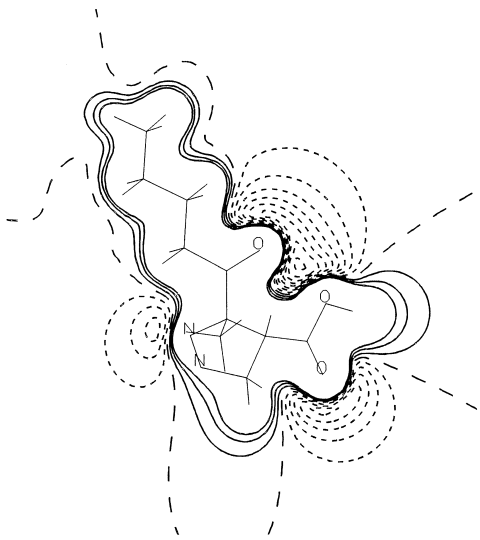

Figure 9. 2-D isopotential map for the fragment **F3** in plane A obtained with ab initio calculations with a 3-21G basis set. Contour details are as in Figure 5. Minimum contour: −80 kcal/mol.

negative potential contours around the aliphatic chain in the lower and middle left of the map could give rise to unfavourable interactions with a lipophilic pocket at the receptor site, as previously hypothesized for other fragments.

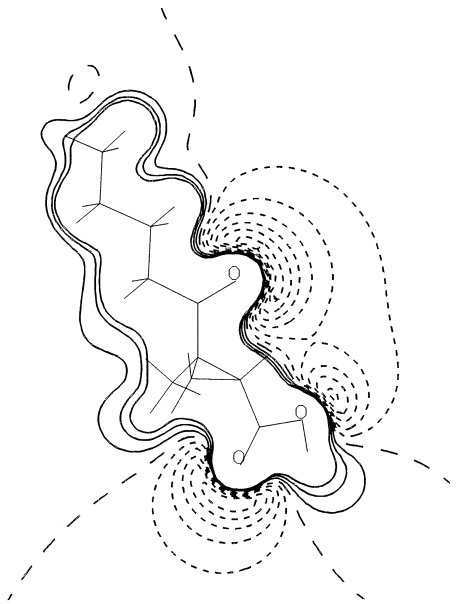

Figure 10. 2-D isopotential map for the fragment **F4** in plane A obtained with ab initio calculations with a 3-21G basis set. Contour details are as in Figure 5. Minimum contour: −60 kcal/mol.

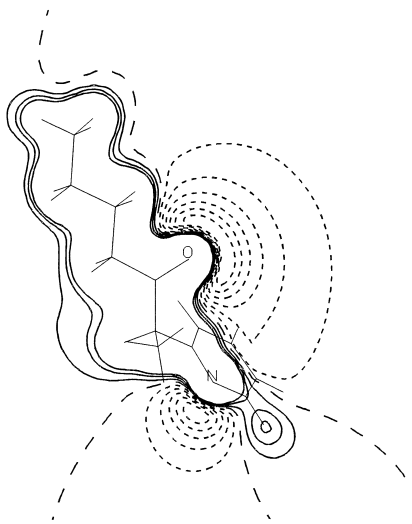

Figure 11. 2-D isopotential map for the fragment **F5** in plane A obtained with ab initio calculations with a 3-21G basis set. Contour details are as in Figure 5. Minimum contour: −60 kcal/mol.

Similarly, many other stable and representative conformers of the acyclic derivatives produce MEP distributions where the electrostatic requirements for binding to the AII receptor could be compromised, especially in the region of the aliphatic chain.

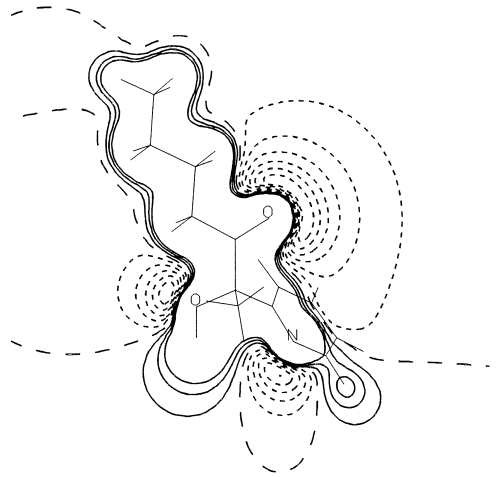

Figure 12. 2-D isopotential map for the fragment **F6** in plane A obtained with ab initio calculations with a 3-21G basis set. Contour details are as in Figure 5. Minimum contour: −60 kcal/mol.

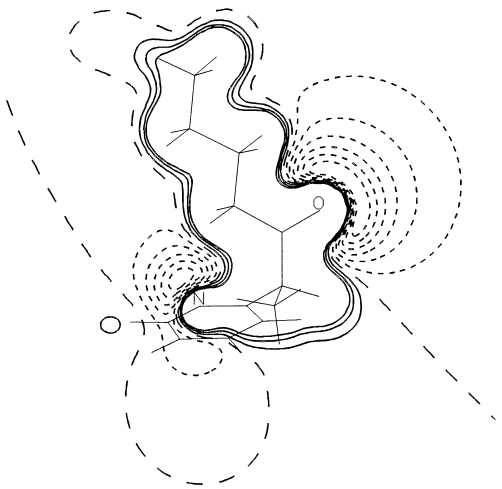

Figure 13. 2-D isopotential map for the fragment **F5** derived from the lowest energy conformer of **5** in plane A obtained with ab initio calculations with a 3-21G basis set. Contour details are as in Figure 5. Minimum contour: −60 kcal/mol.

In conclusion, the novel acyclic imidazole-mimicking units allow the exploration of new structural areas of potential interest in the field of AII receptor antagonism. The conformational and/or electrostatic diversity sampled by the acyl derivatives of Figure 4 is mainly to be ascribed to nonplanar dispositions of the acyclic replacements of the heterocycle moiety. Unfortunately, the pharmacological assays reveal that such structural diversity implies low binding affinity for the AT_1 receptor.

The reason for this behaviour could be found in conformational preferences no longer optimal for receptor interaction and/or responsible for alterations of the electrostatic pattern around the aliphatic chain, whose electronic distribution is crucial to its fitting well with a lipophilic pocket at the receptor site.

The validity of previously derived activity models and the possibility of improvements and refinements emerge from this study: the information provided by structure–activity relationships of the novel acyclic compounds is valuable to gain insight into a better understanding of the molecular requirements for optimal drug–receptor interactions.

Experimental

General. Thin-layer chromatography was performed on silica gel plates (60 F_{254}, Merck). Flash chromatography was performed on silica gel (Kieselgel 60, 230–400 mesh) using the indicated solvent mixture. Melting points were measured with a Büchi 535 apparatus and are uncorrected. ^{1}H and ^{13}C NMR spectra were recorded in $CDCl_3$ at 200 and 50.3 MHz, respectively, with a Bruker AC-200 spectrometer, using TMS as internal standard. The infrared spectra were recorded on a Perkin–Elmer FTIR 1600 spectrometer. The mass spectra were obtained with a VG 7070 EQ-HF mass spectrometer. Gas-chromatography (GLC) was performed on a DANI 3600 gas chromatograph equipped with a flame ionization detector using a glass column filled with chromosorb WHP (D-OV17). Elemental analyses were performed by the microanalytical laboratory of our department.

Diethyl-2-oxo-hexyl-phosphonate (8). To a solution of diethyl methylphosphonate **7** (22.4 g, 147.2 mmol) in dry THF (150 mL) under nitrogen at −78 °C was added *n*-BuLi 1.6 M in hexane (147.2 mmol, 92 mL) and the mixture stirred for 90 min. Ethyl valerate (73.6 mmol, 10.96 mL) was then added and the reaction warmed to room temperature. The mixture was quenched with 200 mL of H_2O and extracted with CH_2Cl_2 (4×100 mL). The combined organic layers were washed with water until neutral pH, dried with Na_2SO_4 and evaporated under reduced pressure. The residue was then distilled at vacuum-pump pressure to afford **8** (14 g, yield 80.5%) as colourless oil, bp 100 °C/1.5 mm. ^{1}H NMR ($CDCl_3$) δ 4.10 (quint, J=6.5 Hz, 4H, OCH_2CH_3), 3.05 (d, J=22.8 Hz, 2H, $COCH_2PO$), 2.60 (t, J=7 Hz, 2H, CH_2CO), 1.55 (quint, J=7 Hz, 4H, $CH_3CH_2CH_2$), 1.30 (t, J=6.5 Hz, 6H, OCH_2CH_3), 0.80 (t, J=7 Hz, 3H, $CH_3CH_2CH_2$). ^{13}C NMR ($CDCl_3$) δ 201.15, 62.50, 43.90, 40.97, 25.15, 22.46, 16.56, 13.75. $C_{10}H_{21}O_4P$ (236.5): calcd C 50.84, H 8.96; found C 50.95, H 8.90.

(±) **Diethyl-1-[[2′-[1-(triphenylmethyl)-1*H*-tetrazol-5-yl][1,1′-biphenyl]-4-yl]methyl]-2-oxo-hexyl-phosphonate (10).** To a suspension in dry THF (30 mL) of NaH in mineral oil 60% (0.209 g, 5.23 mmol) under nitrogen at 0 °C compound **8** (1.23 g, 5.23 mmol) dissolved in dry THF (3 mL) was added dropwise. After 5 min, and at room temperature, compound **9** (1.51 g, 2.7 mmol) dissolved in dry THF (12 mL) was added over 8 h. The reaction was stirred until the dialkylated product appeared in the TLC analysis, it was then quenched with 40 mL of satured aqueous NH_4Cl. The aqueous layer was extracted with CH_2Cl_2 (3×30 mL) and the combined organic layers washed with water until neutral pH, dried with Na_2SO_4 and concentrated under reduced pressure. The residue was purified by flash column chromatography (hexane/AcOEt, 85/15) to afford **10** (0.9 g, yield 47%) as a yellow solid, mp 93–94 °C. ^{1}H NMR ($CDCl_3$) δ 7.95–7.85 (m, 1H, aromatic H), 7.55–7.20 (m, 18H, aromatic H), 7.15–6.80 (m, 4H, aromatic H), 4.20 (m, 4H, OCH_2CH_3), 3.55–3.0 (m, 3H, $ArCH_2CH$), 2.64 (dt, J=17.85, 7.5 Hz, 1H, CH_2HCHCO), 2.10 (dt, J=17.85, 7.5 Hz, 1H, CH_2HCHCO), 1.40–1.10 (m, 10 H, OCH_2CH_3, $CH_3CH_2CH_2$), 0.74 (t, J=7 Hz, 3H, $CH_3CH_2CH_2$). LRMS (FAB^+) m/z 712 [M^+]. $C_{43}H_{45}N_4O_4P$ (712.8): calcd C 72.45, H 6.36, N 7.86; found C 72.48, H 6.23, N 7.77.

***cis*/*trans*-4-Oxo-3-[[2′-[1-(triphenylmethyl)-1*H*-tetrazol-5-yl][1,1′-biphenyl]-4-yl]methyl]-oct-2-enoic-acid ethyl ester (11)/(12).** To a suspension of NaH in mineral oil 60% (120 mg, 3.01 mmol) under nitrogen at 0 °C compound **10** (1.95 g, 2.73 mmol) dissolved in dry THF (25 mL) was added dropwise. After 10 min, and at room temperature, freshly prepared ethyl glyoxylate (474 mg, 4.65 mmol) dissolved in dry THF (2 mL) was added dropwise. The mixture was stirred for 60 h and then quenched with 30 mL of saturated aqueous NH_4Cl, extracted with CH_2Cl_2 (3×30 mL). The combined organic layers were dried with Na_2SO_4 and concentrated under reduced pressure. The residue was purified by flash column chromatography (hexane/AcOEt, 8/2) to afford **11/12** (1.55 g, yield 86%) as mixture of diastereomers **11**(*E*)/**12**(*Z*), 60/40 calculated by NMR experiments.

(*E*) Isomer 11. ^{1}H NMR ($CDCl_3$) δ 8.0–7.80 (m, 1H, aromatic H), 7.62–7.20 (m, 18H, aromatic H), 7.15–6.90 (m, 4H, aromatic H), 6.58 (s, 1H, C=C*H*), 4.30 (q, J=7.5 Hz, 2H, OCH_2CH_3), 4.15 (s, 2H, $ArCH_2$), 2.55 (t, J=8 Hz, 2H, CH_2CO), 1.65–1.20 (m, 7H, OCH_2CH_3, $CH_3CH_2CH_2$), 0.85 (t, J=6.5 Hz, 3H, $CH_3CH_2CH_2$). $C_{43}H_{40}N_4O_3$ (660.8): calcd C 78.16, H 6.10, N 8.48; found C 78.04, H 6.18, N 8.34.

(*Z*) Isomer 12. ^{1}H NMR ($CDCl_3$) δ 8.0–7.80 (m, 1H, aromatic H), 7.62–7.20 (m, 18H, aromatic H), 7.15–6.90

(m, 4H, aromatic H), 5.50 (t, $J=1.25$ Hz, 1H, C=C*H*), 4.15 (q, $J=7.5$ Hz, 2H, OCH_2CH$_3$), 3.45 (d, $J=1.25$ Hz, 2H, ArCH_2), 2.45 (t, $J=8$ Hz, 2H, CH_2CO), 1.65–1.20 (m, 7H, OCH$_2$CH_3, CH$_3$CH_2CH_2), 0.85 (t, $J=6.5$ Hz, 3H, CH_3CH$_2$CH$_2$). $C_{43}H_{40}N_4O_3$ (660.8): calcd C 78.16, H 6.10, N 8.48; found C 78.22, H 6.19, N 8.59.

***trans*-4-Oxo-3-[[2′-(1*H*-tetrazol-5-yl)[1,1′-biphenyl]-4-yl]-methyl]-oct-2-enoic-acid ethyl ester (1b).** A solution of *trans* isomer **11** (0.15 g, 0.227 mmol) in MeOH (3 mL) was refluxed for 4 h. The reaction was then concentrated and the crude product was purified by flash column chromatography (hexane/AcOEt, 8/2 and $CHCl_3$/MeOH, 9/1) to afford **1b** (0.085 g, yield 90%). ^{1}H NMR ($CDCl_3$) δ 8.34–8.20 (m, 1H, aromatic H), 7.64–7.15 (m, 7H, aromatic H), 6.73 (s, 1H, C=C*H*), 4.30 (q, $J=7.5$ Hz, 2H, OCH_2CH$_3$), 3.65 (s, 2H, ArCH_2), 2.62 (t, $J=7.5$ Hz, 2H, CH_2CO), 1.65–1.15 (m, 7H, OCH$_2$CH_3, CH$_3$CH_2CH_2), 0.89 (t, $J=6.5$ Hz, 3H, CH_3CH$_2$CH$_2$). $C_{24}H_{26}N_4O_3$ (418.5): calcd C 68.88, H 6.26, N 13.39; found C 68.71, H 6.19, N 13.47.

(±)-*trans*-3-[[2′-[1-(Triphenylmethyl)-1*H*-tetrazol-5-yl]-[1,1′-biphenyl]-4-yl]methyl]-3-valeryl-4-carbethoxy-1-pyrazoline (13). Alkenes **11/12** (1.55 g, 2.35 mmol) were dissolved in 15 mL of Et_2O at −10 °C and then a solution of CH_2N_2 in diethyl ether was added until the yellow colour permanently appeared in the solution. The flask was wrapped with aluminum foil and the mixture stirred for 2 h at −10 °C and then warmed to room temperature. Only the *E*-isomer reacts (by TLC analysis). The mixture was concentrated under reduced pressure and the residue purified by flash column chromatography (hexane/AcOEt, 8/2) to afford **13** (913 mg, yield 55%) and **12** (440 mg). ^{1}H NMR ($CDCl_3$) δ 8.0–7.80 (m, 1H, aromatic H), 7.62–7.20 (m, 18H, aromatic H), 7.15–6.90 (m, 4H, aromatic H), 4.88 (dd, $J=17$, 6 Hz, 1H, N=NHC*H*), 4.45 (dd, $J=17$, 8 Hz, 1H, N=N*H*CH), 4.15 (q, 2H, OCH_2CH$_3$), 3.25 (dd, $J=8$, 6 Hz, 1H, C*H*COOEt), 3.21 (d, $J=14$ Hz, 1H, ArHC*H*), 3.06 (d, $J=14$ Hz, 1H, Ar*H*CH), 2.25 (t, $J=7$ Hz, 2H, CH_2CO), 1.68–1.10 (m, 7H, OCH$_2$CH_3, CH$_3$CH_2CH_2), 0.75 (t, $J=6.5$ Hz, 3H, CH_3CH$_2$CH$_2$). ^{13}C NMR ($CDCl_3$) δ 207.10, 170.15, 164.27, 142.22, 141.82, 141.22, 138.18, 130.60, 130.15, 129.74, 128.93, 128.15, 127.52, 127.11. $C_{44}H_{42}N_6O_3$ (702.8): calcd C 75.19, H 6.02, N 11.96; found C 75.08, H 6.17, N 11.94.

(±)-*trans*-3-[[2′-(1*H*-Tetrazol-5-yl)[1,1′-biphenyl]-4-yl]-methyl]-3-valeryl-4-carbethoxy-1-pyrazoline (3b). A solution of **13** (0.25 g, 0.356 mmol) dissolved in 40 mL of MeOH was refluxed for 4 h and then the reaction was concentrated. The residue was then recrystallized from ethyl acetate to provide 0.16 g of **3b** (yield 97%), mp 151.4–152.7 °C. ^{1}H NMR ($CDCl_3$) δ 8.20–8.10 (m, 1H, aromatic H), 7.62–7.20 (m, 7H, aromatic H), 4.85 (dd, $J=17$, 8 Hz, 1H, N=NHC*H*), 4.65 (dd, $J=17$, 10 Hz, 1H, N=N*H*CH), 4.15 (q, $J=6.5$ Hz, 2H, OCH_2CH$_3$), 3.75 (d, $J=15$ Hz, 1H, ArHC*H*), 3.45 (dd, $J=10$, 8 Hz, 1H, C*H*COOEt), 3.15 (d, $J=15$ Hz, 1H, Ar*H*CH), 2.60 (m, 2H, CH_2CO), 1.60–1.10 (m, 7H, OCH$_2$CH_3, CH$_3$CH_2CH_2), 0.90 (t, $J=6.5$ Hz, 3H, CH_3CH$_2$CH$_2$). ^{13}C NMR ($CDCl_3$) δ 205.40, 170.86, 154.46, 142.34, 141.82, 141.20, 138.19, 130.56, 130.05, 129.74, 128.95, 128.13, 127.52, 126.45, 106.3, 79.97, 62.12, 41.53, 40.13, 37.97, 25.21, 22.16, 14.0, 13.67. $C_{25}H_{28}N_6O_3$ (460.5): calcd C 65.2, H 6.13, N 18.25; found C 65.23, H 6.15, N 18.21.

(±)-*trans*-2-[[2′-[1-(Triphenylmethyl)-1*H*-tetrazol-5-yl]-[1,1′-biphenyl]-4-yl]methyl]-2-valeryl-cyclopropan-1-carboxylic acid ethyl ester (14). To a solution of **13** (0.65 g, 0.926 mmol) in acetone (2 mL) 300 mL of hexane were added and the mixture was loaded into the photoreactor provided with a quartz sun-lamp (500 W). After 2 h of irradiation the solvent was removed under reduced pressure. The residue was purified by flash column chromatography (hexane/AcOEt, 8/2) to afford **14** (0.34 g, yield 53%) in 9/1 ratio *trans*/*cis*. ^{1}H NMR ($CDCl_3$) δ 8.0–7.80 (m, 1H, aromatic H), 7.62–7.20 (m, 18H, aromatic H), 7.15–6.90 (m, 4H, aromatic H), 4.20–4.0 (m, 2H, OCH_2CH$_3$), 3.29 (s, 2H, ArCH_2), 2.44 (dd, $J=6.5$, 3 Hz, 1H, C*H*COOEt), 2.35 (t, $J=7$ Hz, 2H, CH_2CO), 1.76–1.20 (m, 9H, OCH$_2$CH_3, CH$_3$CH_2CH_2, CH_2CHCOOEt), 0.81 (t, $J=7.5$ Hz, 3H, CH_3CH$_2$CH$_2$). $C_{44}H_{42}N_4O_3$ (674.8): calcd C 78.31, H 6.27, N 8.30; found C 78.35, H 6.23, N 8.23.

(±)-*trans*-2-[[2′-(1*H*-Tetrazol-5-yl)[1,1′-biphenyl]-4-yl]methyl]-2-valeryl-cyclopropan-1-carboxylic acid ethyl ester (4b). A solution of *trans* isomer **14** (0.28 g, 0.415 mmol) in MeOH (20 mL) was refluxed for 4 h. The reaction was then concentrated and the crude product was purified by flash column chromatography (hexane/AcOEt, 8/2 and $CHCl_3$/MeOH, 9/1) to afford **4b** (0.16 g, yield 90%). Successful flash column chromatography with CH_2Cl_2 allowed the isolation of the product. ^{1}H NMR ($CDCl_3$) δ 8.0–6.90 (m, 8H, aromatic H), 4.15 (q, $J=7$ Hz, 2H, OCH_2CH$_3$), 3.29 (dd, $J=15$ Hz, 2H, ArCH_2), 2.44 (dd, $J=6$, 3 Hz, 1H, C*H*COOEt), 2.35 (m, 2H, CH_2CO), 1.70–1.35 (m, 6H, CH$_3$CH_2CH_2, CH_2CHCOOEt), 1.22 (t, $J=7$ Hz, 3H, OCH$_2$CH_3), 0.75 (t, $J=7.5$ Hz, 3H, CH_3CH$_2$CH$_2$). $C_{25}H_{28}N_4O_3$ (432.5): calcd C 69.42, H 6.53, N 12.95; found C 69.45, H 6.59, N 12.88.

(±) 2-(2-Hydroxyhexyl)pyridine (15). To a stirred solution of 2-picoline (10 g, 0.107 mol) in dry THF (70 mL) BuLi 2.5 M in hexane (43 mL, 0.107 mol) was dropped under N_2 atmosphere at −10 °C. The red solution was stirred at 0 °C for 30 min, then a solution of valeraldehyde (11.4 mL, 0.107 mol) in dry THF (30 mL) was added dropwise at 0 °C. The cooling bath was removed. The mixture reached room temperature in 1 h and was

left under stirring for an additional 1 h. The mixture was then cooled to 0 °C and H_2O (40 mL) was added. The pH was adjusted to 2 by adding aqueous HCl. The resulting phases were separated and the aqueous one was extracted with Et_2O (250 mL), cooled to 0 °C and a solution of Na_2CO_3 was added to adjust the pH to 10. The alkaline solution was extracted with Et_2O (200 mL×2). The combined organic layers were washed with brine, dried on Na_2SO_4 and evaporated under reduced pressure. The crude oil (17.6 g) was distilled under vacuum. In the first fraction the unreacted 2-picoline (0.68 g) was recovered. The title product was distilled at 115–124 °C/0.12 mm Hg (g 7.33, 38%). ^{1}H NMR ($CDCl_3$) δ 8.55–8.44 (m, 1H, aromatic H), 7.68–7.52 (m, 1H, aromatic H), 7.18–7.05 (m, 2H, aromatic H), 5.10 (s broad, 1H, O*H*), 4.11–3.93 (m, 1H, C*H*OH), 2.99–2.75 (m, 2H, CH_2Py), 1.70–1.15 (m, 4H, $CH_3CH_2CH_2$), 0.91 (t, J = 6.7 Hz, 3H, $CH_3CH_2CH_2$). GLC assay ≥95%. $C_{11}H_{17}NO$ (179.2): calcd C 73.7, H 9.56, N 7.81; found C 73.65, H 9.48, N 7.78.

2-(2-Oxohexyl)pyridine (16). To a stirred and cooled (15 °C) solution of **15** (6.3 g, GLC assay 91%, 0.032 mol) in acetone (distilled on $KMnO_4$, 10 mL), 96% H_2SO_4 (0.9 mL) was added to obtain a clear solution; H_2O (1 mL) was also added. The temperature was decreased to 10 °C and the Jones reagent (10 mL) was dropped over 20 min, maintaining the temperature lower than 30 °C. The mixture was stirred at room temperature for 2 h. A further amount of Jones reagent (3 mL) was added under cooling. Stirring was continued for an additional hour. The mixture was cooled to 10 °C, added with *i*PrOH and diluted with acetone (100 mL). The insoluble oil was separated by decantation and washed with acetone (40 mL) which was then combined with the previous one. The separated insoluble oil was diluted with H_2O (80 mL) and the pH adjusted to 9 with concentrated NaOH. The aqueous suspension was extracted with Et_2O (40 mL×2). The collected organic extracts were washed with brine, combined with the previously obtained acetone phase, dried on Na_2SO_4 and evaporated under reduced pressure. The residue (4.2 g) was chromatographed (hexane/AcOEt, 50/50) to give the title compound (1.7 g, 30%) as a yellow oil. ^{1}H NMR ($CDCl_3$) δ 8.61–8.51 (m, 1H, aromatic H), 7.72–7.58 (m, 1H, aromatic H), 7.29–7.12 (m, 1H, aromatic H), 3.92 (s, 2H, CH_2Py), 2.54 (t, J = 17.5 Hz, 2H, CH_2CO), 1.70–1.15 (m, 4H, $CH_3CH_2CH_2$), 0.87 (t, J = 7.2 Hz, 3H, $CH_3CH_2CH_2$). GLC assay: 97.4%. $C_{11}H_{15}NO$ (177.2): calcd C 74.54, H 8.53, N 7.90; found C 74.57, H 8.48, N 7.83.

(±)-2-[2-Oxo-1-[[2′-[1-(triphenylmethyl)-1*H*-tetrazol-5-yl]-[1,1′-biphenyl]-4-yl]methyl]hexyl]-pyridine (17). To a stirred and cooled (0 °C) suspension of 80% NaH (0.14 g, 4.64 mmol) in dry THF (7 mL), a solution of **16** (0.95 g, 5.36 mmol) in dry THF (10 mL) was added dropwise, under N_2 atmosphere, over a period of 10 min. The cooling bath was removed and after 10 min a solution of 5-[4′-(bromomethyl)-[1,1′-biphenyl]-2-yl]-1-(triphenylmethyl)-1*H*-tetrazole (2.66 g, ^{1}H NMR assay 76%, 3.57 mmol) was added dropwise to the reaction mixture. The solution was stirred at room temperature for about 8 h and the solvent was then removed in vacuo. The resulting oil was taken up with H_2O, acidified with 5.5 N HCl and extracted with AcOEt (25 mL×2). The combined organic phases were washed in sequence with diluted aqueous HCl solution, 5% $NaHCO_3$, H_2O and brine, dried on Na_2SO_4 and evaporated under reduced pressure. The resulting residue was purified by flash-chromatography (hexane/AcOEt, 60/40) to give the pure product (2.19 g, 94%) as a yellowish spongy powder. ^{1}H NMR ($CDCl_3$) δ 8.54–8.51 (m, 1H, aromatic H), 7.88–7.78 (m, 1H, aromatic H), 7.45–6.75 (m, 25H, aromatic H), 4.10 (t, J = 7.4 Hz, 1H, C*H*Py), 3.38 (dd, J = 7.4, 13.7 Hz, 1H, *H*CHAr), 3.01 (dd, J = 7.4, 13.7 Hz, 1H, HC*H*Ar), 2.42–2.15 (m, 2H, CH_2CO), 1.48–1.25 (m, 2H, $CH_3CH_2CH_2$), 1.20–0.98 (m, 2H, $CH_3CH_2CH_2$), 0.75 (t, J = 7.1 Hz, 3H, $CH_3CH_2CH_2$). $C_{44}H_{39}N_5O$ (653.8): calcd C 80.83, H 6.01, N 10.71; found C 80.75, H 5.97, N 10.80.

(±)-2-[2-Oxo-1-[[2′-[1-(triphenylmethyl)-1*H*-tetrazol-5-yl][1,1′-biphenyl]-4-yl]methyl]hexyl]pyridine-1-oxide (18) and (±)-2-[1-hydroxy-2-oxo-1-[[2′-[1-(triphenylmethyl)-1*H*-tetrazol-5-yl][1,1′-biphenyl]-4-yl]methyl]hexyl] pyridine (19). To a stirred solution of **17** (1.7 g, 2.6 mmol) in CH_2Cl_2 (15 mL), a suspension of *m*-chloroperbenzoic acid (1.08 g, 3.12 mmol) in 5 mL of CH_2Cl_2 was added at room temperature. The stirring was continued for 1.5 h. The reaction solution was then cooled to 5 °C and 5% $NaHCO_3$ (10 mL) was added. The phases were separated and the organic one was washed with brine, dried on Na_2SO_4 and evaporated under reduced pressure. The resulting residue (1.8 g) was chromatographed. The higher R_f compound **19** (0.7 g) was obtained as a spongy whitish powder using a mixture of hexane/AcOEt (70/30) as eluent. Further elution with CH_2Cl_2/MeOH (90/10) gave the title compound **18** (0.34 g, 20%) as a yellowish powder.

Alcohol 18. ^{1}H NMR ($CDCl_3$) δ 8.28–8.18 (m, 1H, aromatic H), 7.92–7.80 (m, 1H, aromatic H), 7.51–7.18 (m, 12H, aromatic H), 7.12–6.82 (m, 13H, aromatic H), 4.53 (t, J = 7.7 Hz, 1H, C*H*Py), 3.28 (dd, J = 7.7, 13.7 Hz, 1H, *H*CHAr), 3.07 (dd, J = 7.7, 13.7 Hz, 1H, HC*H*Ar), 2.64–2.48 (m, 1H, *H*CHCO), 2.23–2.04 (m, 1H, HC*H*CO), 1.65–1.08 (m, 4H, $CH_3CH_2CH_2$), 0.79 (t, J = 7.0 Hz, 3H, $CH_3CH_2CH_2$). MS (FAB$^+$) *m/e* 670 (MH^+). IR (nujol) ν 1712 cm^{-1} (C=Ostr). $C_{44}H_{39}N_5O_2$ (669.8): calcd C 78.9, H 5.87, N 10.46; found C 78.87, H 5.90, N 10.50.

N-Oxide 19. ^{1}H NMR ($CDCl_3$) δ 8.47–8.37 (m, 1H, aromatic H), 7.86–7.76 (m, 1H, aromatic H), 7.72–7.08 (m, 16H, aromatic H), 7.02–6.75 (m, 9H, aromatic H), 5.99 (s, 1H, O*H*), 3.31 (dd, J = 13.6 Hz, 2H, ArCH_2), 2.73–2.32 (m, 2H, CH_2CO), 1.48–1.02 (m, 4H, $CH_3CH_2CH_2$), 0.76 (t, J = 7.0 Hz, 3H, $CH_3CH_2CH_2$). MS (FAB$^+$) *m/e* 670 (MNa$^+$). IR (nujol) ν 1712 cm^{-1} (C=O str). $C_{44}H_{39}N_5O_2$ (669.8): calcd C 78.9, H 5.87, N 10.46; found C 78.83, H 5.89, N 10.41.

(±)-2-[2-Oxo-1-[[2′-(1*H*-tetrazol-5-yl)[1,1′-biphenyl]-4-yl]methyl]hexyl]pyridine (5). A solution of **17** (0.4 g, 0.612 mmol) in MeOH (4 mL) was refluxed for 9 h. The solvent was evaporated under vacuum and the residue was dissolved in Et_2O (8 mL). After a few minutes a precipitate appeared. The suspension was stirred for 1 h. The solid was then filtered off, washed with Et_2O and dried to constant weight to give the title compound (0.22 g, 88%) as a white powder, mp 134–137 °C (with dec.). ^{1}H NMR ($CDCl_3$) δ 8.64–8.42 (m, 1H, aromatic H), 8.07–7.98 (m, 1H, aromatic H), 7.78–7.68 (m, 1H, aromatic H), 7.71–7.18 (m, 5H, aromatic H), 6.84 (m, 4H, aromatic H), 4.08 (dd, J = 5.8, 9.3 Hz, 1H, C*H*Py), 3.33 (dd, J = 5.8, 13.7 Hz, 1H, *H*CHAr), 3.03 (dd, J = 9.3, 13.7 Hz, 1H, HC*H*Ar), 2.32 (t, J = 7.15 Hz, 2H, CH_2CO), 1.53–1.35 (m, 2H, $CH_3CH_2CH_2$), 1.28–1.06 (m, 2H, $CH_3CH_2CH_2$), 0.80 (t, J = 7.1 Hz, 3H, $CH_3CH_2CH_2$). $C_{25}H_{25}N_5O$ (411.5):calcd C 72.97, H 6.12, N 17.02; found C 72.89, H 6.05, N 17.09.

The following compounds were analogously prepared.

(±)-2-[2-Oxo-1-[[2′-(1*H*-tetrazol-5-yl)[1,1′-biphenyl]-4-yl]methyl]hexyl]-pyridine-1-oxide (20). Starting from **18** (0.28 g, 0.418 mmol) the crude product was obtained (0.28 g). It was purified by flash chromatography using at the first hexane/AcOEt (50/50) and then CH_2Cl_2/MeOH/AcOH (90/9.5/0.5). The fractions containing the compound were evaporated in vacuo and the residue was partitioned between H_2O and AcOEt. The pH was adjusted to 7 by adding diluted aqueous $NaHCO_3$ solution. The layers were separated and the aqueous one extracted with AcOEt. The combined organic layers were washed with brine, dried on Na_2SO_4 and evaporated under reduced pressure to obtain the pure compound (0.15 g, 83.7%) as a yellowish spongy powder. ^{1}H NMR ($CDCl_3$) δ 8.22–8.11 (m, 1H, aromatic H), 7.91–7.78 (m, 1H, aromatic H), 7.58–7.15 (m, 6H, aromatic H), 6.98–6.78 (m, 4H, aromatic H), 4.95–4.75 (m, 1H, C*H*Py), 3.31 (dd, J = 9.85, 13.5 Hz, 1H, *H*CHAr), 3.01 (dd, J = 5.65, 13.5 Hz, HC*H*Ar), 2.51–2.21 (m, 2H, CH_2CO), 1.55–1.32 (m, 2H, $CH_3CH_2CH_2$), 1.30–1.05 (m, 2H, $CH_3CH_2CH_2$), 0.79 (t, J = 7.1 Hz, $CH_3CH_2CH_2$). ^{13}C NMR ($CDCl_3$) δ 206.98, 155.05, 149.08, 141.16, 139.73, 137.89, 137.82, 137.12, 131.12, 130.79, 130.57, 129.11, 128.02, 126.25, 125.09, 123.20, 53.11, 42.44, 35.98, 25.63, 22.15, 13.86. $C_{25}H_{25}N_5O_2$ (427.5): calcd C 70.24, H 5.89, N 16.38; found C 70.30, H 5.94, N 16.33.

(±)-2-[1-Hydroxy-2-oxo-1-[[2′-(1*H*-tetrazol-5-yl)[1,1′-biphenyl]-4-yl]methyl]hexyl]-pyridine (6). Starting from **19** (0.25 g, 0.373 mol) the title compound was obtained (0.12 g, 75%) as a yellowish spongy powder, after purification performed as described above. ^{1}H NMR ($CDCl_3$) 8.61–8.51 (m, 1H, aromatic H), 8.32–8.21 (m, 1H, aromatic H), 7.82–7.18 (m, 6H, aromatic H), 7.08 (m, 4H, aromatic H), 3.47 (dd, J = 13.5 Hz, 2H, ArCH_2), 2.85–2.65 (m, 1H, *H*CHCO), 2.55–2.32 (m, 1H, HC*H*CO), 1.51–1.05 (m, 4H, $CH_3CH_2CH_2$), 0.79 (t, J = 7.0 Hz, 3H, $CH_3CH_2CH_2$). ^{13}C NMR ($CDCl_3$) 212.97, 156.71, 154.48, 147.69, 141.00, 137.55, 137.47, 136.71, 131.37, 130.67, 130.51, 128.34, 123.37, 122.22, 121.10, 83.53, 44.36, 37.47, 25.48, 22.12, 13.82. $C_{25}H_{25}N_5O_2$ (427.5): calcd C 70.24, H 5.89, N 16.38; found C 70.17, H 5.97, N 16.43.

Acknowledgements

We wish to thank Dr. A. R. Renzetti (Laboratori Guidotti related to A. Menarini, Industrie Farmaceutiche Riunite) for binding studies and Mr. S. Bettoni for technical assistance. The work was supported by C.N.R. (Progetto Finalizzato Chimica Fine), and by a European Community grant (HCM Program-A2, contract No. ERBCHRXCT 920027). The authors are also grateful to Professor W. C. Still for the use of the program MacroModel and to Molecular Design Ltd. for the use of the program REACCS.

References and Notes

1. Valloton, M. B. *Trends Pharmacol. Sci.* **1987**, *8*, 69.

2. Carini, D. J.; Duncia, J. V.; Aldrich, P. E.; Chiu, A. T.; Johnson, A. L.; Pierce, M. E.; Price, W. A.; Santella III, J. B.; Wells, G. J.; Wexler, R. R.; Wong, P. C.; Yoo, S. E.; Timmermans, P. B. M. W. M. *J. Med. Chem.* **1991**, *34*, 2525.

3. Christen, Y.; Waeber, B.; Nussberger, J.; Prochet, M.; Borland, R. M.; Lee, R. J.; Maggon, K.; Shum, L.; Timmermans, P. B. M. W. M.; Brunner, M. R. *Circulation* **1991**, *83*, 1271.

4. Greenlee, W. J.; Mantlo, N. B., Eds. *Bioorg. Med. Chem. Lett.* **1994**, *4*, entire issue.

5. Salimbeni, A.; Canevotti, R.; Paleari, F.; Bonaccorsi, F.; Renzetti, A.R.; Belvisi, L.; Bravi, G.; Scolastico, C. *J. Med. Chem.* **1994**, *37*, 3928, and references cited therein.

6. Salimbeni, A.; Canevotti, R.; Paleari, F.; Poma, D.; Caliari, S.; Fici, F.; Cirillo, R.; Renzetti, A. R.; Subissi, A.; Belvisi, L.; Bravi, G.; Scolastico, C.; Giachetti, A. *J. Med. Chem.* **1995**, *38*, 4806, and references cited therein.

7. Cirillo, R.; Renzetti, A. R.; Cucchi, P.; Guelfi, M.; Salimbeni, A.; Caliari, S.; Castellucci, A.; Evangelista, S.; Subissi, A.; Giachetti, A. *Br. J. Pharmacol.* **1995**, *114*, 1117.

8. Belvisi, L.; Bravi, G.; Scolastico, C.; Vulpetti, A.; Salimbeni, A.; Todeschini, R. *J. Comput.-Aided Mol. Des.* **1994**, *8*, 211.

9. Belvisi, L.; Bonati, L.; Bravi, G.; Pitea, D.; Scolastico, C; Vulpetti, A. *J. Mol. Struct. (TEOCHEM)* **1993**, *281*, 237.

10. Bühlmayer, P.; Furet, P.; Criscione, L.; De Gasparo, M.; Whitebread, S.; Schmidlin, T.; Lattmann, R.; Wood, J. *Bioorg. Med. Chem. Lett.* **1994**, *4*, 29.

11. Belvisi, L.; Bravi, G.; Catalano, G.; Mabilia, M.; Salimbeni, A.; Scolastico, C. *J. Comput.-Aided Mol. Des.* **1996**, *10*, 567.

12. Todeschini, R.; Marengo, E. *Chemom. Intell. Lab. Syst.* **1992**, *16*, 25.

13. Chang, G.; Guida, W. C.; Still, W. C. *J. Am. Chem. Soc.* **1989**, *111*, 4379.

14. Burkert, U.; Allinger, N. L. *Molecular Mechanics*; ACS Monograph 177: Washington, DC, 1982.

15. Ponder, W. J.; Richards, F. M. *J. Comput. Chem.* **1987**, *8*, 1016.

16. Mohamadi, F.; Richards, N. G. J.; Guida, W. C.; Liskamp, R.; Caufield, C.; Chang, G.; Hendrickson, T.; Still, W. C. *J. Comput. Chem.* **1990**, *11*, 440.

17. An 8 kcal/mol cutoff was arbitrarily chosen in our first 3-D QSAR study[8] to ensure a large representative sampling of populated minima for the conformationally flexible antagonists under investigation. In the present work the same cutoff was adopted to be in keeping with the previous study and to properly use the geometrical activity model.

18. Frisch, M. J.; Head-Gordon, M.; Trucks, G. W.; Foresman, J. B.; Schlegel, H. B.; Raghavachari, K.; Robb, M. A.; Binkley, J. S.; Gonzalez, C.; Defrees, D. J.; Fox, D. J.; Whiteside, R. A.; Seeger, R.; Melius, C. F.; Baker, J.; Martin, R. L.; Kahn, L. R.; Stewart, J. J. P.; Topiol, S.; Pople, J. A. *GAUSSIAN 90*, Gaussian Inc., Pittsburgh, PA, 1990.

19. *SURFER V4*, Golden Software, Golden, CO.

20. Ford-Moore, A. H.; Perry, B. J. *Organic Syntheses*, Collect. IV, 325.

21. Wadsworth, W. S.; Emmons, W. D. *J. Am. Chem. Soc.* **1961**, *83*, 1733.

22. Jung, M. E.; Shishido, K.; Davis, L. M. *J. Org. Chem.* **1982**, *47*, 891.

23. Feringa, B. L.; De Lange, B.; De Jong, J. C. *J. Org. Chem.* **1989**, *54*, 2471.

24. Carrié, R. *Heterocycles* **1980**, *14*, 1529.